

# Geostrophic currents in the central part of the Red Sea during early summer

Geostrophy currents  
Red Sea  
Courants géostrophiques  
Été  
Mer Rouge

Salman SULTAN, Fazal AHMAD

Faculty of Marine Science, King Abdulaziz University, 21441 Jeddah, P.O. Box 1540, Saudi Arabia.

Received 24/4/89, in revised form 14/12/89, accepted 20/12/89.

## ABSTRACT

Computation of geostrophic currents in the Red Sea along a latitudinal transverse between 21 and 22°N in early summer indicate a northward drift on the western and a southward drift along the eastern side. The mean of the depth-mean average northward currents is 7.7 cm/s, giving a northward transport of  $1.9 \times 10^6$  m<sup>3</sup>/s, from the coast of Sudan to approximately 38°22'E. To the east of that, towards the Arabian coast, there is a southward current of 14 cm/s giving a transport of  $2.1 \times 10^6$  m<sup>3</sup>/s. The direct current measurements at three depths from a mooring line near the eastern side of the Red Sea also show a southward drift which decreases with depth.

*Oceanologica Acta*, 1990. 13, 3, 397-401.

## RÉSUMÉ

### Courants géostrophiques au centre de la mer Rouge

Les courants géostrophiques calculés le long d'une section transversale de la mer Rouge entre 21 et 22°N indiquent la présence au début de l'été d'une dérive vers le nord le long de la côte occidentale et d'une dérive vers le sud le long de la côte orientale. Avec une vitesse moyenne à mi-profondeur de 7,7 cm/s, le transport vers le nord est de  $1,9 \cdot 10^6$  m<sup>3</sup>/s, entre la côte du Soudan et 38°22'E. Le long de la côte d'Arabie, le courant dirigé vers le sud, à une vitesse de 14 cm/s, donne un flux de  $2,1 \cdot 10^6$  m<sup>3</sup>/s. Les mesures de courant effectuées à trois profondeurs, sur une ligne ancrée près de la côte orientale, montrent que la dérive vers le sud diminue lorsque la profondeur augmente.

*Oceanologica Acta*, 1990. 13, 3, 397-401.

## INTRODUCTION

Currents in the southern region, particularly the strait of Bab-el-Mandab, are relatively well known in comparison with the remainder of the Red Sea (Patzert, 1974). In the central Red Sea at about 20°N, the surface currents are in a northwest direction during winter (Barlow, 1934). A subsurface counter-current flows southward at a depth greater than 250 m in the open sea and less than 150 m near the coast of Sudan. Maillard (1971) showed, from geostrophic analysis, that the currents during February were variable and generally transversal. From winter hydrographic data between 24 and 28°N, Boisvert (1966) and Bibik (1968) interpreted the presence of a large cyclonic eddy. Luksch (1901) also showed the existence of cyclonic circulations from the temperature and salinity observations of the "Pola" expedition. Mohammad (1940) supported Luksch's conclusions. Morcos (1970) states that "the currents flowing in the axial direction represent, according to the region and time of observation, from 22-30 % of all currents".

Both thermohaline forcing and wind are responsible for generating circulation in the Red Sea (Maury, 1855; Thompson, 1939 *a, b*; Neumann and McGill, 1962; Phillips, 1966; Siedler, 1969; Patzert, 1972; Gerges and Soliman, 1982; Wassef *et al.*, 1983). In early summer the winds are less uniform (Phillips, 1966; Patzert, 1974) and it is generally admitted (Maillard and Soliman, 1986) that the main driving force is buoyancy. The present study is based on data from hydrographic stations extending along the width of the central Red Sea (Fig. 1). The geostrophic computation of data at two stations yields the current component perpendicular to the line between the two stations. From the discussion of the hydrographic structure perpendicular to the north-northwest/south-southeast axis of the Red Sea, Neumann and McGill (1962) showed that lateral variations are transient and can be ignored.

## DATA ANALYSIS

Data from six hydrographic stations 26, 25, 24, 20, 22, 28, between latitudes 21-22° in the central region of

the Red Sea, were analysed for geostrophic currents (Fig. 1). These data were collected during an environmental survey carried out by the Saudi/Sudanese Commission for the Exploitation of the Red Sea Resources by the survey vessel *Soela* in mid-May 1978. A digital CTD probe (Guildline Model 8705) was used to measure conductivity ratio ( $\pm 0.0004$ ), temperature ( $\pm 0.02^\circ\text{C}$ ) and pressure ( $\pm 1\%$ ). Temperature and salinity were read at standard depth intervals and averages of lowering and raising values are used for calculating the dynamic heights. (Figs. 2 A, B, C, D) show the vertical sections of temperature, salinity,  $\sigma_t$  and computed geostrophic speed respectively along the latitudinal transverse. The surface temperature is lower in the central part of the section and increases towards the western and eastern coasts. In the central Red Sea, the surface temperature is at its minimum ( $< 25^\circ\text{C}$ ) in February and increases from March onwards. The ther-

mocline begins to develop during this period (Patzert 1972). The bottom water below 700 m is characterized by a potential temperature of  $21.59 \leq T^\circ\text{C} \leq 21.66$  and a salinity of  $40.55 \leq S \leq 40.58$  and the reference level can therefore safely be placed at this level. The computed current velocities are significantly small at greater depths, so the depth-mean averages (average velocity between the depth intervals multiplied by the interval and divided by the sum of the intervals) only down to 200 m are considered.

Direct current records from Aanderaa current meters were available from a mooring-line ( $21^\circ 25.5' \text{N}$ ,  $38^\circ 6.1' \text{E}$ ) at depths of 52, 109 and 181 m in a water depth of 1940 m. These data were recorded every 20 minutes (23-31 May 1978) by the Saudi/Sudanese Commission during the Environmental Survey Programme. Twenty-minute speed and direction data were smoothed to obtain hourly values. The transient and

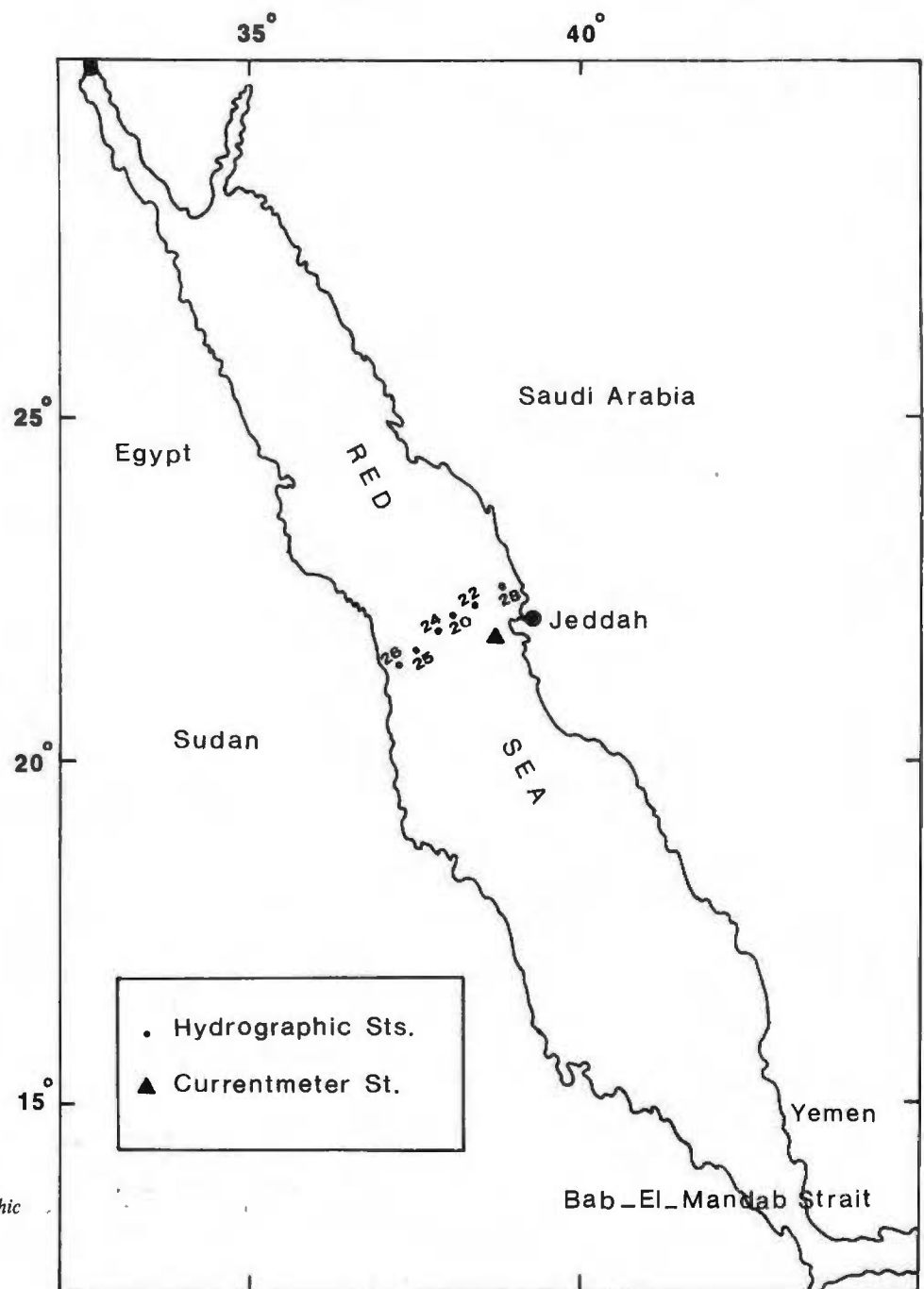


Figure 1  
Map of the Red Sea showing hydrographic and current meter stations.

tidal components of the velocity spectrum were removed by applying a 25-hour mean filter. Stick plots of the residual component of velocity are shown in Figure 3. During this period the average current velocities at the above-mentioned depths were about 35, 34 and 8 cm/s respectively. It is clear that the dominant direction at the three depth levels is east-northeast and that the velocity decreases with depth.

**ERROR ANALYSIS**

The error in the computation of dynamic height is directly proportional to the error in the determination of the specific volume anomaly and to the distance from the reference level to the given isobar. Computation of currents by the dynamic method requires that the reference level be located in the no-motion layer. Retaining this requirement and considering the accuracy of the dynamic method, the error in the computed dynamic height may become comparable to the actual dynamic height if the reference level is located at greater depth. In this case it is sensible to place the reference level at a depth where computational errors will not influence the reliability of the results. Based on this consideration and the availability of tempera-

ture and salinity data with depth, the reference level was established at 700 m. The measuring accuracy of the conductivity ratio ( $\pm 0.0004$ ) and temperature ( $\pm 0.02^\circ\text{C}$ ) with the CTD probe introduces an approximate error of  $0.015 \sigma_t$  units. Therefore the error in the specific volume anomaly will be approximately  $1.6 \times 10^{-5} \delta$  units. The maximum error in the computation of dynamic height  $\Delta D$  with 700 m as the level of no motion is  $700 \times 1.4 \times 10^{-5}$  which averages to about 10 per cent of the calculated specific volume anomaly. This leads to an approximate error of  $\pm 0.6$  cm/s in velocity and about 8% in transport.

**RESULT AND DISCUSSIONS**

Depth-mean average velocities between stations 26-25, 25-20, 24-22, and 22-28 are 10.0, 8.3, 4.7 and 14.0 cm/s respectively. Between the first three pairs of stations the drift is to the north; between stations 22-28, it is to the south. The mean of the depth-mean currents to the north is 7.7 cm/s and that to the south is 14.0 cm/s. From station 22, the coasts of Sudan and Arabia are at distances of 125 and 75 km respectively. Application of these widths gives a northward transport of

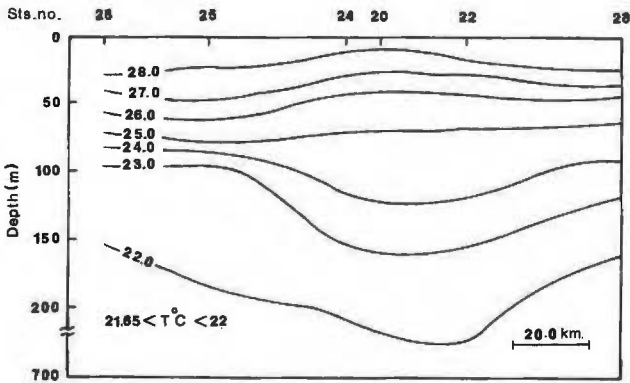


Figure 2 A  
Vertical section of temperature contours every 1°C.

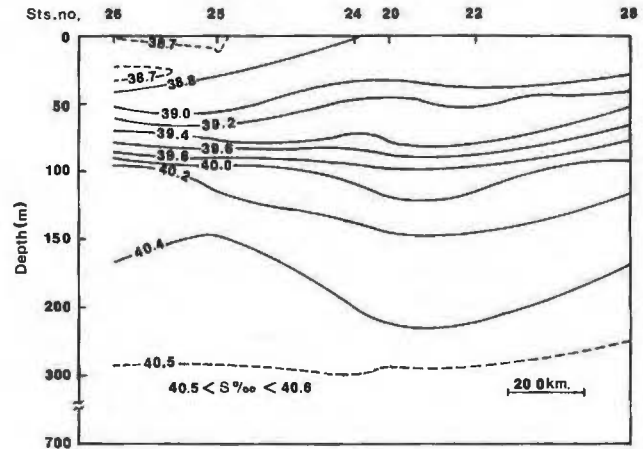


Figure 2 B  
Vertical section of salinity contours every 0.2‰.

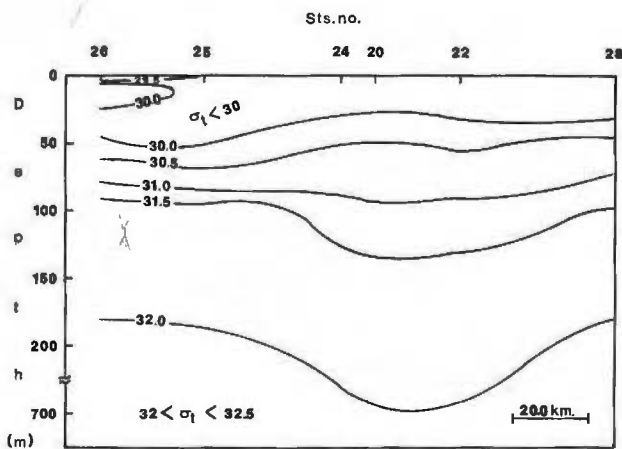


Figure 2 C  
Vertical section of density contours every 0.5  $\sigma_t$ .

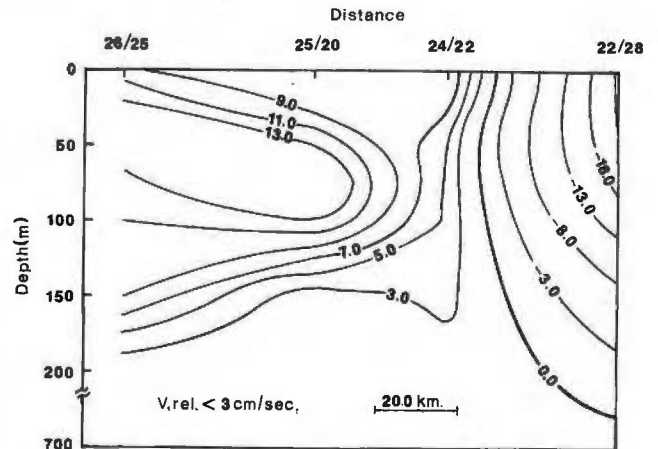


Figure 2 D  
Vertical section of geostrophic speed in cm/s.

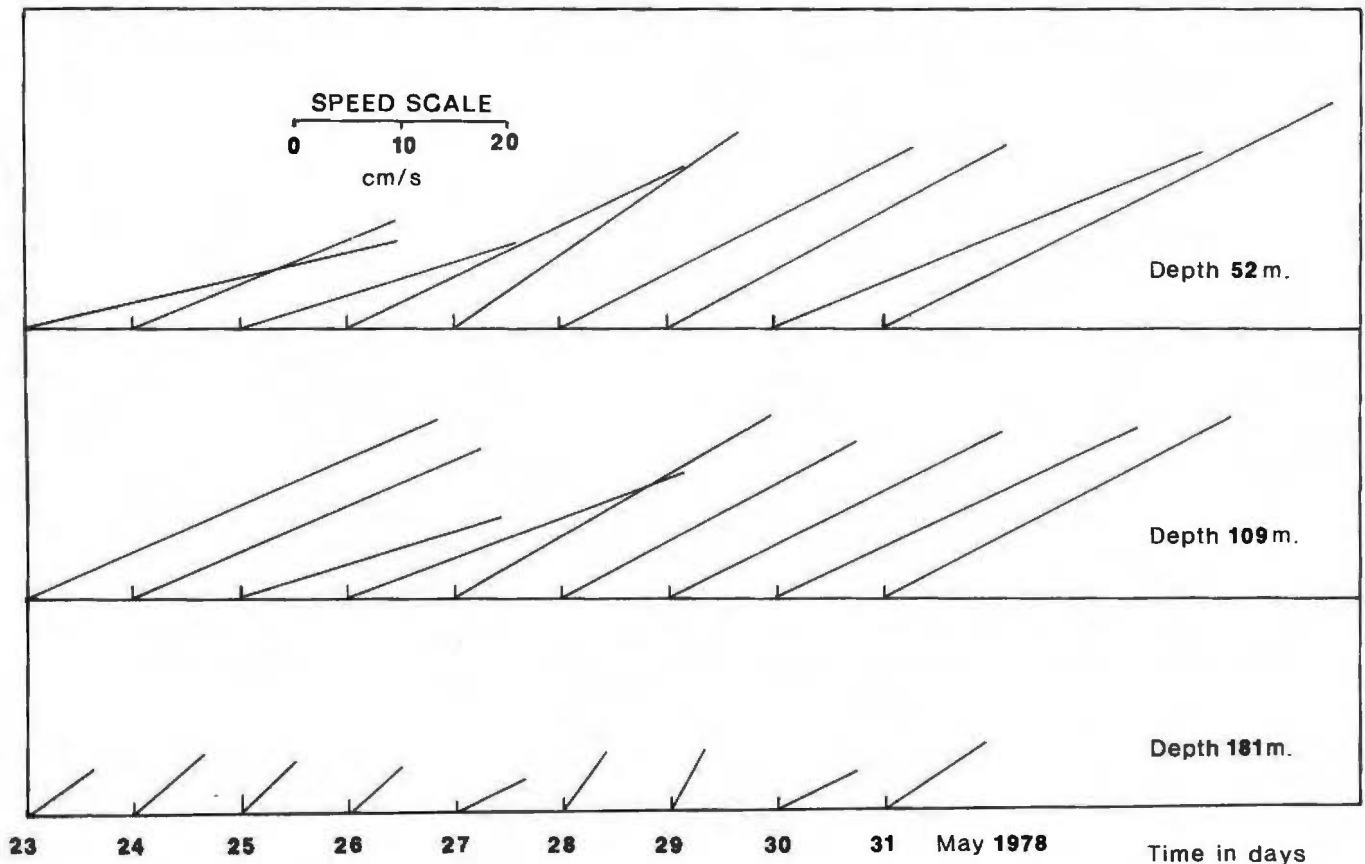


Figure 3  
Stick plots of residual velocity at different depths.

$1.9 \times 10^6 \text{ m}^3/\text{s}$  and a southward transport of  $2.1 \times 10^6 \text{ m}^3/\text{s}$ . Northward and southward transport rates seem to be in agreement with each other, within the error of the field observations or calculations. The variations of temperature, salinity and  $\sigma_t$  are mainly in the upper 200 m (Figs. 2 A, B, C). Below this depth the deep water mass is almost homogeneous and is characterized by

$$21.65^\circ \leq T^\circ\text{C} \leq 22^\circ;$$

$$40.5 \leq S^\circ/\text{‰} \leq 4.6 \quad \text{and} \quad 32.3 \leq \sigma_t \leq 32.5.$$

The isolines indicate downwelling near the centre of the section. This may be associated with an anticyclonic motion shown by the geostrophic computation (Fig. 2D). Analysis of data from current-meter moorings at 52, 109 and 181 m depths shows that the velocities are 35, 34 and 8 cm/s respectively. The dominant direction during this period is east-northeast. The

decrease in velocity below 100 m is quite rapid. Therefore it would be expected that the velocity at 700 m, which is the level of no motion, will be near zero. The geostrophic velocities at the corresponding levels are 22, 15 and 1 cm/s. These velocities are considerably lower than the direct measurements. This is to be expected, as the geostrophic method gives only a component of velocity perpendicular to the line joining the stations.

#### Acknowledgements

We extend our sincere thanks to the Saudi/Sudanese Commission for the Exploitation of the Red Sea Resources, for making available the hydrographic data. Thanks are also due to Mr. S. Al-Nady, to Mr. A. Al-Barakati for drawing the diagrams and to Mr. A. Azzoghhd for typing the manuscript.

## REFERENCES

- Barlow E. W.** (1934). Currents of the Red Sea and part of the Indian Ocean north of Australia. *Marine Observer*, **110**, 67-68; **110**, 150-154.
- Bibik V. A.** (1968). Peculiarities of the hydrological conditions in the northern part of the Red Sea in winter season of 1964-1965, *Okeanologicheskie Issledovania*, No. **15**, pp. 45-68 (in russian).
- Boisvert W. W.** (1966). Ocean currents in the Arabian Sea and northeast Indian Ocean. Naval Oceanographic office Rep. SP-92; 12 charts.
- Gerges M. A. and G. F. Soliman** (1982). Principal feature of circulation in the Red Sea as obtained from a two-layer mathematical model. Proceedings of the International Conference on Marine Sciences, Red Sea, El-Gardaga; Egypt.
- Luksch J.** (1901). Expedition S.M. "Pola" in das Rothe Meer. *Deutsch. Akad. Wiss. XVIII Physikal Untersuchungen*, **LXIX**, 337-98.
- Muhamad A. F.** (1940). The Egyptian Exploration of the Red Sea. *Proc. Soc., Lond., Ser. B*, **128**, 306-316.
- Mauzy M. F.** (1855). The physical geography of the sea and its meteorology. Edited by John Leighly, The Harvard Library, Cambridge, Mass. (1966), 432 pp.
- Maillard C.** (1971). Étude hydrologique et dynamique de la Mer Rouge en hiver d'après les observations du Commandant Robert Giraud (1963). Thèse présentée à la Faculté des Sciences de Paris pour l'obtention du Doctorat de 3<sup>e</sup> cycle. 77 pp.
- Maillard C. and G. Soliman** (1986). Hydrography of the Red Sea and exchanges with the Indian Ocean in summer, *Oceanologica Acta*, **9**, 3, 249-269.
- Morcos S. A.** (1970). Physical and chemical oceanography of the Red Sea. *Oceanography and Marine Biology Annual Review* volume **8**, 73-202.
- Neumann A. C. and D. A. McGill** (1962). Circulation of the Red Sea in early summer. *Deep-Sea Res.*, **8**, 223-235.
- Patzert W. C.** (1972). Seasonal variation in structure and circulation in the Red Sea. Ph. D. Thesis Hawaii, Institute of Geophysics. University of Hawaii.
- Patzert W. C.** (1974). Wind induced reversal in Red Sea circulation. *Deep-Sea Res.*, **21**, 109-121.
- Phillips O. M.** (1966). On turbulent convection currents and the circulation of the Red Sea. *Deep-Sea Res.*, **13**, 1149-1160.
- Siedler G.** (1969). General circulation of water masses in the Red Sea. in: *Hot Brines and Recent Heavy Metal Deposits in the Red Sea*. E. T. Degens and D. A. Ross (eds), Springer-Verlag, New York, Inc., 131-137.
- Thompson E. F.** (1939) *a*. Chemical and physical investigations. The general hydrography of the Red Sea. John Murray Expedition 1933-34. *Scientific Reports*, **2**, (3), 83-103.
- Thompson E. F.** (1939) *b*. Chemical and physical investigations. The exchange of water between the Red Sea and the Gulf of Aden over the "Sill". John Murray Expedition 1933-34. *Scientific Reports*, **2**, (4), 105-119.
- Wassef R. K., M. A. Gerges and G. F. Soliman** (1983). Wind driver circulation in the Red Sea as a homogeneous basin. *Bulletin of the Institute of Oceanography and Fisheries*, Cairo, **9**.

